Optical Production of Ultracold Polar Molecules

Jeremy M. Sage,[1] Sunil Sainis,[1] Thomas Bergeman,[2] and David DeMille[1]

[1] *Department of Physics, Yale University, New Haven, CT 06520, USA*
[2] *Department of Physics and Astronomy, SUNY, Stony Brook, NY 11794-3800, USA*

(Dated: January 3, 2022)

We demonstrate the production of ultracold polar RbCs molecules in their vibronic ground state, via photoassociation of laser-cooled atoms followed by a laser-stimulated state transfer process. The resulting sample of $X^1\Sigma^+(v = 0)$ molecules has a translational temperature of ~ 100 μK and a narrow distribution of rotational states. With the method described here it should be possible to produce samples even colder in all degrees of freedom, as well as other bi-alkali species.

PACS numbers: 33.80.Ps, 39.25.+k, 33.80.Wz, 33.70.Ca

Samples of ultracold, polar molecules (UPMs) can provide access to new regimes in many phenomena. Ultracold temperatures allow trapping, and polarity can be used to engineer large, anisotropic, and tunable interactions between molecules. These features make UPMs attractive as qubits for quantum computation [1], as building blocks for novel types of many-body systems [2], and for the study of chemistry in the ultracold regime [3]. Furthermore, UPMs can be used as uniquely sensitive probes of phenomena beyond the Standard Model of particle physics [4].

Methods such as buffer-gas cooling [5], Stark-slowing [6], billiard-like collisions [7], and velocity filtering [8] have produced samples of polar molecules at temperatures of $\sim$ 10–100 mK. Formation of heteronuclear molecules from pre-cooled atoms via photoassociation (PA) [9, 10, 11, 12] or Feshbach resonance techniques [13] promises access to much lower temperatures; however, these processes leave molecules in highly excited vibrational levels, which have vanishingly small polarity [14] and are unstable to collisions [15, 16]. The possibility of transferring such molecules to their vibronic ground state, via optical processes such as stimulated Raman transitions, has been discussed extensively (see e.g. [1, 17, 18, 19, 20]); however, insufficient data on the structure of experimentally accessible molecules has made it difficult to identify specific pathways for efficient transfer.

Here we report the production of UPMs via PA of laser-cooled Rb and Cs atoms, followed by a two-step stimulated emission pumping (SEP) process. This yields RbCs molecules in their absolute vibronic ground state $X^1\Sigma^+(v = 0)$. These polar molecules (calculated electric dipole moment $\mu \approx 1.3$ D [21]) have a translational temperature of $\sim$100 μK. The distribution of rotational states is also quite narrow, so the resulting sample of $X^1\Sigma^+$ state molecules is cold in all degrees of freedom.

Figure 1 shows the methods by which we produce and detect UPMs. A pair of colliding, ultracold Rb and Cs atoms is photoassociated, i.e., the pair absorbs a photon and is driven to an electronically excited molecular level [22]. This level decays rapidly, with branching fraction of $\sim 7\%$ into the long-lived $a^3\Sigma^+(v = 37)$ level [9]. After a period of PA, a resonant laser pulse ("pump" pulse) transfers these metastable, vibrationally excited molecules to an intermediate, electronically excited state (i). The population of state i is monitored by applying an intense laser pulse ("ionization" pulse), with a frequency chosen to selectively form a $RbCs^+$ molecular ion. We detect these ions using time-of-flight mass spectroscopy.

To produce $X(v = 0)$ molecules, a second tunable laser pulse ("dump" pulse), arriving just after the pump pulse, resonantly drives molecules in state i to the $X(v = 0)$ (or, for diagnostic purposes, $v = 1$) state. Transfer to the $X(v = 0, 1)$ states is indicated by a depletion of the i state population. This method [23] generally works well, but is complicated by the presence of additional resonant features associated with transitions from state i upward into other, spectrally uncharacterized excited states.

We thus employ a second method to directly detect the RbCs $X(v = 0, 1)$ molecules. After the dump pulse, the population of state i is allowed to decay for several times its spontaneous emission lifetime, leaving essentially no population in this level. Next a third pulse ("re-excitation" pulse), identical in frequency to the dump, drives the stable $X^1\Sigma^+(v = 0, 1)$ molecules back into state i, where they are detected via ionization as before. The ion signal is monitored as the frequency of the identical dump and re-excitation pulses is scanned; a peak in this signal indicates that molecules have been resonantly transferred to the $X^1\Sigma^+(v = 0, 1)$ states by the dump pulse, then back to the i state by the re-excitation pulse. The definitive signatures of UPM production are resonances at the exact frequencies predicted by earlier spectroscopy of the $a^3\Sigma^+$, i [9, 18], and $X^1\Sigma^+$ levels [24].

The state i is in the manifold of levels associated with the overlapping electronic states $c^3\Sigma^+$, $b^3\Pi$, and $B^1\Pi$. Specifically, the states chosen for i have predominantly $c^3\Sigma_1^+$ character, with small admixtures of $b^3\Pi_1$ (due to non-adiabatic couplings of the potentials) and $B^1\Pi_1$ (due to spin-orbit coupling). The mixed c/B state composition of i is crucial to the technique (the small b state admixture is incidental). The $c^3\Sigma^+$ component of the i state has reasonable Franck-Condon (FC) overlap

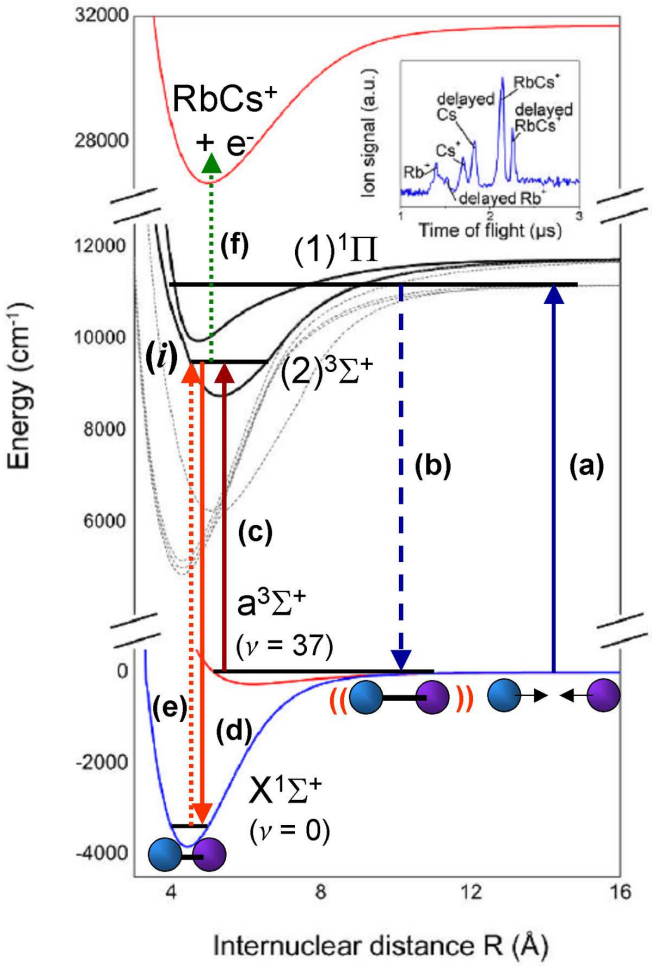

FIG. 1: (color online) Formation and detection processes for ultracold ground state RbCs. (a) Colliding atom pairs are excited into weakly bound RbCs* molecules, which (b) decay prominently into the $a^3\Sigma^+(v = 37)$ state. (c) Metastable $a(v = 37)$ molecules are excited to level i, then (d) stimulated down into the $X^1\Sigma^+(v = 0)$ state. The molecules are detected directly by (e) driving them back to the original excited level and (f) ionizing them, or indirectly by detecting the depletion of the i level population (where only (f) is needed). Inset: a typical time-of-flight mass spectrum showing the direct detection of $X(v = 0)$ molecules. The ion signal, averaged over 200 shots, is plotted vs. delay time after the ionizing pulse. The delayed $RbCs^+$ peak signifies ground state molecule production.

with the initial $a^3\Sigma^+(v = 37)$ state, due to the near-coincidence of the inner turning point of the $a^3\Sigma^+$ potential with the minimum of the $c^3\Sigma^+$ potential [9, 18]. The $B^1\Pi$ component of state i circumvents the usual selection rule forbidding transitions from the initial triplet state a to the final singlet state X. Moreover, the minima of the $B^1\Pi$ and $X^1\Sigma^+$ potentials nearly coincide, leading to large FC factors for transfer to the $X(v = 0)$ level.

The apparatus is similar to that described in our earlier work [9]. Briefly, ^{85}Rb and ^{133}Cs atoms were cooled and collected in a dual-species, forced dark SPOT magneto-optical trap (MOT) [25, 26, 27]. The atomic density n and atom number N were $n_{\rm Rb} = 1 \times 10^{11}$ cm^{-3}, $N_{\rm Rb} = 2 \times 10^8$, and $n_{\rm Cs} = 3 \times 10^{11}$ cm^3, $N_{\rm Cs} = 3 \times 10^8$. The temperature of both species was $\sim$75 μK. The atoms were photoassociated by a Ti:Sapphire laser with intensity of $\sim$ 3 kW/m^2. Its frequency was locked to an $\Omega = 0^-$, $J^P = 1^+$ level, located 38.02 cm^{-1} below the Rb $5S_{1/2}(F = 2)$ + Cs $6P_{1/2}(F = 3)$ atomic asymptote.

All other laser light consisted of pulses with $\sim$ 5 ns duration and $\sim$ 3 mm diam. The pump pulse was generated from a tunable dye laser operating from 18100–18600 cm^{-1} at a 10 Hz repetition rate with a spectral linewidth of $\sim$0.05 cm^{-1}. This output was sent through a H_2 Raman cell; the second Stokes order (down-shifted by 2×4155.25 cm^1) was separated to form the pump pulse, with a typical intensity of 20 J/m^2 and frequency from 9800-10300 cm^{-1}. The dump and re-excitation pulses were generated using an additional dye laser (the "red" laser) operating from 13500-14000 cm^{-1} with a spectral linewidth of $\sim$0.2 cm^{-1}; each had a typical intensity of 3 J/m^2. The ionizing pulse (at 532 nm) was derived from the second harmonic of the Nd:YAG laser used to pump the dye lasers, and had an intensity of 100 J/m^2.

The red and ionizing beams were spatially combined using a dichroic mirror with the ionizing pulse propagating 4 ns behind the red pulse. These combined beams were sent through a beam splitter. In one half of the split two-color beam, the optical path length was adjusted such that the red dump pulse reached the molecules 7 ns after the pump pulse. The other half of the two-color beam was sent through a 22 m long multimode optical fiber; with this delay, the red re-excitation pulse arrived 110 ns after the dump pulse.

Laser frequencies were measured using a wavelength meter with 0.05 cm^{-1} accuracy. Ions were detected using a channeltron located $\sim$3 cm from the atoms. The digitized channeltron current yields a time-of-flight mass spectrum, as shown in the inset of Fig. 1. The temperature of the molecules in the $a^3\Sigma^+$ state was measured as described in Ref. [8]. The scattering of two photons necessary to transfer the population to the $X(v = 0)$ state should not cause significant heating.

For a particular choice of state i, we scanned the frequency of the red laser through the predicted energy splitting between the chosen level and the $X^1\Sigma^+(v = 0, 1)$ states. We observed transfer to the ground states via several of these levels. Results are shown for three such intermediate states i, consecutive in energy, in Fig. 2.

The locations of the resonant features are in excellent agreement with the known $X(v = 0) - (v = 1)$ splitting [24], and with our measured splitting of the i state levels. In Fig. 2c, a scan over the region between the $v = 0$ and $v = 1$ resonances shows features only at the predicted locations. As a cross-check, we also deliberately chose as state i the $\Omega = 0^-$ component of a mixed $c^3\Sigma^+/b^3\Pi$ level.

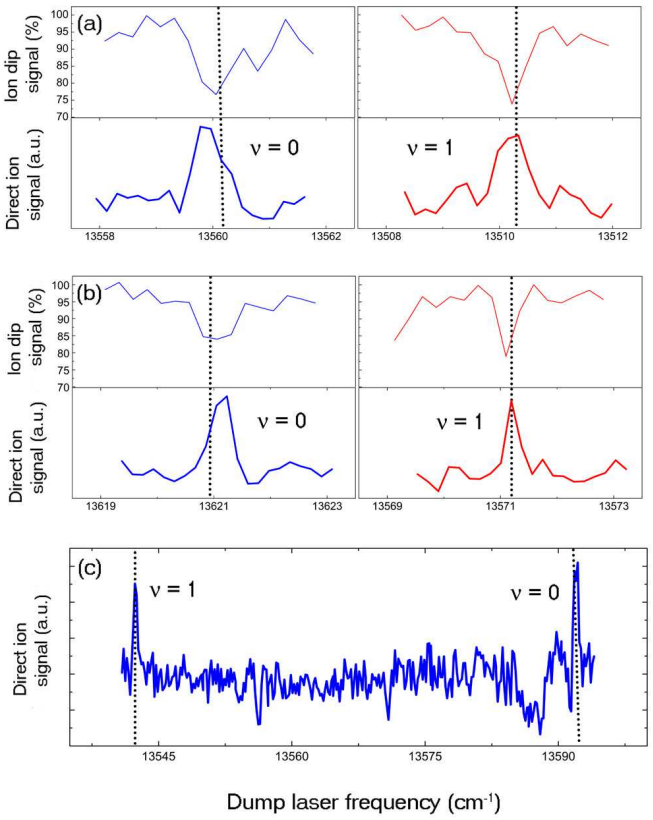

FIG. 2: (color online) Observation of $X^1\Sigma^+(v = 0, 1)$ state molecules. Results are shown for i state depletion (upper) and direct detection (lower) for three consecutive states i, located at energies of (a) 9754.26 cm^{-1}, (b) 9814.60 cm^{-1}, and (c) 9786.10 cm^{-1} above the $a^3\Sigma^+(v = 37)$ state. In (c), the region between the $v = 0$ and $v = 1$ resonances is shown to have no additional features for direct detection. The dotted lines indicate the predicted dump laser frequency for the desired transition.

Here, selection rules rigorously prevent coupling to the $X^1\Sigma^+$ state, and as expected we observe no evidence for transfer. Finally, we determined the strength of the $i-X$ transitions by increasing the red laser intensity until the resonant features broadened. The observed saturation intensities (typically ~ 4 J/m^2) agree qualitatively with those predicted from calculated FC factors and electronic transition moments [18].

Presently, we detect ~ 1 ion per pulse. This indicates a production rate of $\sim 2 \times 10^2$ UPMs/s, subject to uncertainties in the channeltron gain and ionization efficiency. Based on the agreement between observed and predicted rates, this figure should be correct to within a factor of ~ 2. The UPM production rate is suboptimal for a few reasons. First, MOT densities were not optimized for this work. Second, the molecules are untrapped, and most leave the region before our low repetition-rate lasers can transfer them. Finally, the efficiency of the SEP is only $\sim 6\%$. This is determined by the measured $\sim 25\%$ dump and re-excitation efficiencies and our inference of a similar pump efficiency (due to the comparable red and pump laser linewidths). This low value is expected due to the sparse comb-like spectral structure typical of pulsed lasers with multiple longitudinal modes [28], such as that used here. This structure implies that we would need to broaden the transitions considerably in order to achieve the theoretical maximum 25% transfer efficiency for SEP with our current lasers.

By changing our experimental conditions in straightforward ways, the method described here can lead to large rates of UPM production. Thirty-fold higher $a(v = 37)$ production rates could be achieved by returning to our optimized MOT conditions [9]. Using higher repetition rate pulsed lasers and/or trapping the RbCs molecules could lead to $\sim 100\%$ addressing of the vibrationally excited molecules. Finally, using a stimulated Raman adiabatic passage (STIRAP) technique with transform-limited laser pulses [29, 30], the $a(v = 37)$ to $X(v = 0)$ transfer efficiency would be $\sim 100\%$. With these improvements, we project that the formation rate of RbCs $X(v = 0)$ molecules could approach 3×10^6/s.

Our $X^1\Sigma^+$ molecular sample is of high purity with respect to the vibrational degree of freedom. State i is dominantly triplet in character and thus the probability of uncontrolled spontaneous decay to the $X^1\Sigma^+$ state during the SEP step is extremely small. Using our earlier analysis of the mixed $c/B/b$ state structure [18], we calculated branching ratios for decay of the i states. While these calculations are only qualitative (due our incomplete knowledge of the relevant state wavefunctions), they indicate that the total population in all other vibrational levels of the $X^1\Sigma^+$ state is only $\sim 1\%$ of the population driven into the $v = 0$ level. (Of course, there remains a substantial background of $a^3\Sigma^+$ molecules.)

The rotational and hyperfine state distribution of the $X(v = 0)$ molecules is determined by selection rules and by the spectral resolution of our lasers. Hyperfine structure (hfs) is unresolved in all stages of the process, and hence the nuclear spin degrees of freedom are completely unconstrained. However, the initial PA step selects a level with well-defined rotation/parity quantum numbers $J^P = 1^+$. The three subsequent photons involved in the transfer to the X state (one in spontaneous emission and two in the SEP process) must leave the molecule in a state of odd parity, and can add up to 3 units of angular momentum. Noting that $P = (-1)^J$ for the $X^1\Sigma^+$ state, this suggests that only $J = 1, 3$ could be populated in $X(v = 0)$. However, in principle the molecule can also acquire rotational angular momentum from the nuclear spins, if the coupling between hfs and rotation is sufficiently strong [31]. This can add up to $I_{Rb} + I_{Cs} = 6$ units of rotation (here I_x is the nuclear spin of species x). If this coupling is present, the range of rotational states populated could increase to $J = 1, 3, 5, 7, 9$.

We derive an experimental bound on the spread of populated rotational levels from the absence of large spectral

shifts of the observed resonances from their predicted $J = 0$ locations. Our observations deviate by no more than 0.3 cm^{-1} from these predictions, which have an uncertainty of ± 0.6 cm^{-1} [18]. Using the known rotational constant $B_e = 0.017\,\mathrm{cm}^{-1}$ [24], we conclude that at most, $J = 1, 3, 5$, and 7 are populated.

The spectral width of the dump and re-excitation resonances suggests an even narrower rotational distribution. A typical linewidth of 0.18 cm^{-1} (obtained by subtracting, in quadrature, our laser linewidth from the measured resonance width) agrees well with the predicted 0.17 cm^{-1} splitting between the $J = 1$ and 3 levels. This suggests that the hfs/rotation coupling may be absent (or weak), and that indeed only two rotational levels ($J = 1, 3$) are populated in our experiments.

In future work, we expect to produce molecules in a single rotational level by using transform-limited laser pulses capable of resolving rotational structure. (Such narrowband lasers are required in any case for efficient STIRAP transfer to $X(v = 0)$). State selection of hfs may also be possible by the use of spin-polarized atoms plus judicious choices of laser polarizations and hfs-resolved transitions for PA and state transfer. This would also further increase the rate of $X(v = 0)$ molecule production, since currently the spread of population among hfs sublevels in the $a(v = 37)$ state limits the fraction available for transfer to the i state.

Finally, we point out that this method for UPM production is quite general. Mixing of the $c^3\Sigma^+$ and $B^1\Pi$ levels, as well as the favorable location of the potential curves, is present in all bi-alkali dimers [19]. Although such spin-orbit mixing increases with the mass of the molecules [33], it may be sufficiently large even for the lightest heteronuclear bi-alkali (LiNa). Also, the SEP method is fairly insensitive to the initial vibrational state and completely insensitive to molecular temperature. Thus, higher phase space densities of UPMs could be produced by photoassociating colder atoms or by starting with molecules formed by Feshbach resonance in a single $a^3\Sigma^+$ level [13].

In summary, we have produced ultracold polar RbCs molecules in their ground vibronic state. The optical transfer technique used here should be applicable to other bi-alkali molecules. Translational temperatures limited only by atomic cooling methods should be achievable. The rotational distributions are limited only by laser spectral linewidth; with commonly available technology, population of a single rovibronic state with high purity should be possible. This opens a route to the study and manipulation of polar molecules in the ultracold regime.

We thank A.J. Kerman for crucial contributions to earlier stages of this work and R.C. Hilborn for the loan of essential equipment. We acknowledge support at Yale from NSF Grant DMR0325580, the David and Lucile Packard Foundation, and the W.M. Keck Foundation; and at Stony Brook from NSF grant PHY0354211 and the U.S. Office of Naval Research.

[1] D. DeMille, Phys. Rev. Lett. **88**, 067901 (2002).
[2] M. A. Baranov *et al.*, Phys. Rev. A **66**, 013606 (2002); K. Goral, L. Santos, and M. Lewenstein, Phys. Rev. Lett. **88**, 170406 (2002).
[3] E. Bodo, F. A. Gianturco, and A. Dalgarno, J. Chem. Phys. **116**, 9222 (2002).
[4] M. Kozlov and L. Labzowsky, J. Phys. B **28**, 1933 (1995); J. J. Hudson *et al.*, Phys. Rev. Lett. **89**, 023003 (2002); D. DeMille, Bull. Am. Phys. Soc. **49**, 97 (2004).
[5] J.D. Weinstein et al., Nature (London) **395**, 148 (1998).
[6] H. L. Bethlem *et al.*, Nature (London) **406**, 491 (2000).
[7] M. S. Ellioff, J. J. Valentini, and D. W. Chandler, Science **302**, 1940 (2003).
[8] S. A. Rangwala *et al.*, Phys. Rev. A **67**, 043406 (2002).
[9] A. J. Kerman *et al.*, Phys. Rev. Lett. **92**, 153001 (2004).
[10] M. W. Mancini *et al.*, Phys. Rev. Lett. **92**, 133203 (2004).
[11] C. Haimberger *et al.*, Phys. Rev. A. **70**, 021402(R) (2004).
[12] D. Wang *et al.*, Phys. Rev. Lett. **93**, 243005 (2004).
[13] S. Inouye *et al.*, Phys. Rev. Lett. **93**, 183201 (2004); C. A. Stan *et al.*, Phys. Rev. Lett. **93**, 143001 (2004).
[14] S. Kotochigova, P. S. Julienne, and E. Tiesinga, Phys. Rev. A **68**, 022501 (2003).
[15] V. A. Yurovsky *et al.*, Phys. Rev. A **62**, 043605 (2000).
[16] T. Mukaiyama *et al.*, Phys. Rev. Lett. **92**, 180402 (2004).
[17] B. Damski *et al.*, Phys. Rev. Lett. **90**, 110401 (2003).
[18] T. Bergeman *et al.*, Eur. Phys. J. D **31**, 179 (2004).
[19] W. C. Stwalley, Eur. Phys. J. D **31**, 221 (2004).
[20] S. Kotochigova, E. Tiesinga, and P. S. Julienne, Eur. Phys. J. D **31**, 189 (2004).
[21] G. Igel-Mann *et al.*, J. Chem. Phys. **84**, 5007 (1986); S. Kotochigova, private communication.
[22] H. R. Thorsheim, J. Weiner, and P. S. Julienne, Phys. Rev. Lett. **58**, 2420 (1987); for a review, see: F. Masnou-Seeuws and P. Pillet, Adv. At. Mol. Opt. Phys. **47**, 53 (2001).
[23] D. E. Cooper, C. M. Klimcak, and J. E. Wessel, Phys. Rev. Lett. **46**, 324 (1981).
[24] C. E. Fellows *et al.*, J. Mol. Spectrosc. **197**, 19 (1999).
[25] A. J. Kerman *et al.*, Phys. Rev. Lett. **92**, 033004 (2004).
[26] W. Ketterle *et al.*, Phys. Rev. Lett. **70**, 2253 (1993).
[27] M. H. Anderson *et al.*, Phys. Rev. A **50**, R3597 (1994).
[28] Th. Weber, E. Riedle, and H. J. Neusser, J. Opt. Soc. Am. B **7**, 1875 (1990).
[29] G. He *et al.*, J. Opt. Soc. Am. B **7**, 1960 (1990).
[30] R. Sussman, R. Neuhauser, and H. J. Neusser, J. Chem. Phys. **100**, 4784 (1994).
[31] Strong hfs/rotation coupling requires that hfs be large compared to rotational splittings. This cannot occur in the $X^1\Sigma^+$ or $\Omega = 0^-$ PA states, where the small hfs [24, 25] arises only from electric quadrupole effects. However, strong hfs/rotation coupling could occur in the $a^3\Sigma^+$ and $c^3\Sigma^+$ states, where magnetic dipole hfs is present [32]. Crude estimates indicate that hfs might exceed rotational splittings for low-J levels in these states.
[32] C.H. Townes and A.L. Schawlow, *Microwave Spectroscopy* (McGraw-Hill, New York, 1955).
[33] H. Lefebvre-Brion and R. W. Field, *The Spectra and*

Dynamics of Diatomic Molecules (Elsevier, San Diego, 2004).